3D Anisotropic Diffusion for Liver Segmentation

Wan Nural Jawahir Wan Yussof and Hans Burkhardt

Abstract—Liver segmentation is the first significant process for liver diagnosis of the Computed Tomography. It segments the liver structure from other abdominal organs. Sophisticated filtering techniques are indispensable for a proper segmentation. In this paper, we employ a 3D anisotropic diffusion as a preprocessing step. While removing image noise, this technique preserve the significant parts of the image, typically edges, lines or other details that are important for the interpretation of the image. The segmentation task is done by using thresholding with automatic threshold values selection and finally the false liver region is eliminated using 3D connected component. The result shows that by employing the 3D anisotropic filtering, better liver segmentation results could be achieved eventhough simple segmentation technique is used.

Keywords—3D Anisotropic Diffusion, non-linear filtering, CT Liver.

I. INTRODUCTION

IN the recent years, liver segmentation from Computed Tomography (CT) scans has gain a lot of importance in the field of medical image processing since the composition of liver is vital component in diagnosis of liver disease, surgery planning and therapy control [2], [4], [6]. Automatic liver segmentation is required in today's challenging clinical environment to replace the manual task which is extremely time consuming especially for measurement of three dimensional structures.

Due to the large variability in appearance, size and shape of liver, an automated liver segmentation is still a challenging task. In addition, there is ambiguity of liver boundary and the complex context of nearby organs such as kidney, heart and muscles. Further difficulties arises because quantum noise corrupts the projections in CT at the detector. This noise propagates through the reconstruction to the final volume slices.

To improve the reliability of automatic segmentation algorithms, denoising techniques are required to be used as a preprocessing step. The most basic approach is to apply linear filter. Since CT images have important and structured high frequency components like edges and small details, linear filters such as those used in bandpass, highpass and lowpass are not suitable because they degrade these important structures. Nonlinear filter should be used instead. Each data point is considered separately and either assigned to noise or to a valid structure. If the point is noise, it is simply removed and replaced by an estimate based on surrounding data points. Parts of the data that are not considered noise are not modified at

all. Linear filters lack such a decision capability and therefore modify all data.

In this paper, we describe a 3D anisotropic diffusion that can be employed to carry out the segmentation task. This technique is a non-linear filter used as a preprocessing step. The remaining steps are concerned with subsequent image segmentation of the resulting smoothed images. We calculated the histogram of the 3D filtered image to automatically select the threshold values and finally using 3D connected component to find the largest organ that is regarded as a liver organ.

II. ANISOTROPIC DIFFUSION

Anisotropic diffusion is currently one of the most powerful noise reduction techniques in the field of computer vision. This technique takes into account the local structures found in the image to filter noise, preserve edges and enhance some features.

Pioneered in 1990 by Perona and Malik [5], anisotropic diffusion is also called Perona-Malik equation. The method is based on the numerical solution of nonlinear partial differential equation on two dimensions image. The method is then extended into three dimensions by Gerig et. al in [3]. In this method, smoothing is modeled as a diffusion that is allowed along homogeneous regions and inhibited by region boundaries. The partial differential equation used to describe the diffusion process is the following:

$$\frac{\partial}{\partial t}I(\mathbf{v},t) = \mathbf{div}(c(\mathbf{v},t)\nabla I(\mathbf{v},t)) \quad (1)$$

where $\mathbf{div}$ is a divergence operator and ∇ is a gradient operator. I in our case is the 3D volume of CT image and $\mathbf{v} = (z, y, x)$ is the coordinate vector.

Writing $f = (f_x, f_y, f_z)$, the divergence of vector-valued function f is given by the formula:

$$\mathbf{div}f = \frac{\partial f_x}{\partial x} + \frac{\partial f_y}{\partial y} + \frac{\partial f_z}{\partial z} \quad (2)$$

and the gradient of a scalar function f is defined as:

$$\nabla f = \left[\frac{\partial f}{\partial x}, \frac{\partial f}{\partial y}, \frac{\partial f}{\partial z}\right] \quad (3)$$

Finally, the divergence of ∇f can be written as:

$$\mathbf{div}(\nabla f) = \frac{\partial}{\partial x}\left(\frac{\partial f}{\partial x}\right) + \frac{\partial}{\partial y}\left(\frac{\partial f}{\partial y}\right) + \frac{\partial}{\partial z}\left(\frac{\partial f}{\partial z}\right) \quad (4)$$

At each voxel, the diffusion strength is controlled by the so-called diffusion coefficient $c(\mathbf{v}, t)$ with t is the process ordering parameter used to enumerate iteration steps. The diffusion coefficient $c(\mathbf{v}, t)$ depends on the image gradient magnitude ∇I. It should decrease where the gradient magnitude increases so that image regions of high contrast undergo less diffusion, whereas uniform regions are diffused with the same

W.N.J.W. Yussof is with the Chair for Pattern Recognition and Image Processing, Albert-Ludwigs-Universität Freiburg, Georges-Köhler-Allee 52, Freiburg, 79110 GERMANY e-mail: yussof@informatik.uni-freiburg.de.

H. Burkhadrt is the director of the Chair for Pattern Recognition and Image Processing, Albert-Ludwigs-Universität Freiburg, Georges-Köhler-Allee 52, Freiburg, 79110 GERMANY e-mail:Hans.Burkhadrt@informatik.uni-freiburg.de.

intensity in all directions. Hence the edges can be preserved while removing noise from the image. Two different diffusion functions have been suggested in [5]:

$$c_1(\mathbf{v}, t) = \exp\left(-\left(\frac{|\nabla I(\mathbf{v}, t)|}{\kappa}\right)^2\right) \tag{5}$$

$$c_2(\mathbf{v}, t) = \frac{1}{1 + \left(\frac{|\nabla I(\mathbf{v}, t)|}{\kappa}\right)^2} \tag{6}$$

In this work, $c_1(\mathbf{v}, t)$ is used. This is reported in [3], where c_1 possesses a much stronger edge enhancing capacity than c_2. The parameter κ controls the sensitivity to edges and is chosen as a function of the noise in the image.

A. Filtering of 3D CT Images

The formulation of a 3D diffusion process follows directly from the 2D diffusion process in [3] but the node is now taken from 3D neighborhood of volume elements. This increased number of nodes results in much better noise reduction and in an enhancement of 3D discontinuities, which allows a more accurate preservation of the continuity of structures in 3D space. The following equation is the discrete implementation of 3D procedure which considers only the six immediate neighbors (Fig. 1). However, in our work 26 voxels within a 3x3x3 voxel window are considered.

In order to solve the differential equation, a discrete approximation for the first order derivative is required:

$$\frac{\partial f_x}{\partial x} = \frac{f(x + \Delta x) - f(x)}{\Delta x} \tag{7}$$

$$\frac{\partial f_x}{\partial x} = \frac{f(x) - f(x + \Delta x)}{\Delta x} \tag{8}$$

where Eq. 7 is the forward difference equation and Eq. 8 is the backward difference equation, respectively. The combination of forward difference and backward difference produces central difference. Hence, the formula becomes:

$$\frac{\partial f_x}{\partial x} = \frac{f(x + \frac{1}{2}\Delta x) - f(x - \frac{1}{2}\Delta x)}{\Delta x} \tag{9}$$

Using the approximation equation from Eq. 9 and the divergence of ∇f from Eq. 4, Eq. 1 can be restated as in Eq. 10. It can be solved in an iterative way as follows:

$$I(\mathbf{v}, t + \Delta t) = I(\mathbf{v}, t) + \Delta t \frac{\partial}{\partial t} I(\mathbf{v}, t) \tag{11}$$

The integration constant Δt determines the iterative approximation of stability. It must be adjusted to the different neighborhood structures. As long as Δt is sufficiently small, the iteration scheme expressed in Eq. 11 is stable. Simple analysis to find bounds for the integration constant Δt can be found in [3] where for 3D the maximum Δt for six neighborhoods and 26 neighborhoods are $1/7$ and $3/44$, respectively.

III. LIVER VOLUME SEGMENTATION

A. Thresholding

The distribution of the voxel intensities holds significant information about the 3D image content. Relying on anatomical knowledge regarding the liver volume, information contained in the image histogram can be used to find the initial liver

$$\frac{\partial}{\partial t} I(\mathbf{v}, t) = \mathbf{div}\left[c(\mathbf{v}, t) * \nabla I(\mathbf{v}, t)\right]$$

$$= \nabla^T \left[c(\mathbf{v}, t) * \nabla I(\mathbf{v}, t)\right]$$

$$= \frac{\partial}{\partial x}\left[c(\mathbf{v}, t) * \frac{\partial}{\partial x} I(\mathbf{v}, t)\right)$$

$$+ \frac{\partial}{\partial y}\left(c(\mathbf{v}, t) * \frac{\partial}{\partial y} I(\mathbf{v}, t)\right)$$

$$+ \frac{\partial}{\partial z}\left(c(\mathbf{v}, t) * \frac{\partial}{\partial z} I(\mathbf{v}, t)\right]$$

$$= \frac{1}{\Delta x^2}\left[c\left(x + \frac{\Delta x}{2}, y, z, t\right)\right.$$

$$* \left(I(z, y, x + \Delta x, t) - I(z, y, x, t)\right)$$

$$- c\left(z, y, x - \frac{\Delta x}{2}, t\right) * \left(I(z, y, x, t)\right.$$

$$\left.\left. - I(z, y, x - \Delta x, t)\right)\right]$$

$$+ \frac{1}{\Delta y^2}\left[c\left(z, y + \frac{\Delta y}{2}, x, t\right)\right.$$

$$* \left(I(z, y + \Delta y, x, t) - I(z, y, x, t)\right)$$

$$- c\left(z, y - \frac{\Delta y}{2}, x, t\right) * \left(I(z, y, x, t)\right.$$

$$\left.\left. - I(z, y - \Delta y, x, t)\right)\right]$$

$$+ \frac{1}{\Delta z^2}\left[c\left(z + \frac{\Delta z}{2}, y, x, t\right)\right.$$

$$* \left(I(z + \Delta z, y, x, t) - I(z, y, x, t)\right)$$

$$- c\left(z - \frac{\Delta z}{2}, y, x, t\right) * \left(I(z, y, x, t)\right.$$

$$\left.\left. - I(z - \Delta z, y, x, t)\right)\right] \tag{10}$$

tissues. From a priori knowledge, liver is the largest tissue in the CT image.

To obtain the initial liver region, we propose to perform a thresholding. In Fig. 2, the normalized histogram of 3D image from anisotropic diffusion result is provided. Four peaks are shown corresponding to (a)background, (b) muscle, (c) liver and (d) bones. Notice that, the global maximum corresponds to the background and the peak with the highest local maximum corresponds to the liver tissue. The selection of appropriate thresholds is done by extracting two local minimum between this peak. Voxels whose intensity falls between these two thresholds are assigned as liver region. Otherwise there are assigned as background region (0 value).

B. 3D Connected Component

Due to the fact that some organs in CT image shares similar intensities, there are several organs still remain after
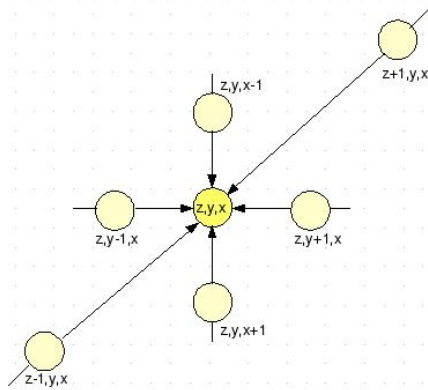
Fig. 1: 3D network structure using six connectivity. Circles represents voxel nodes.
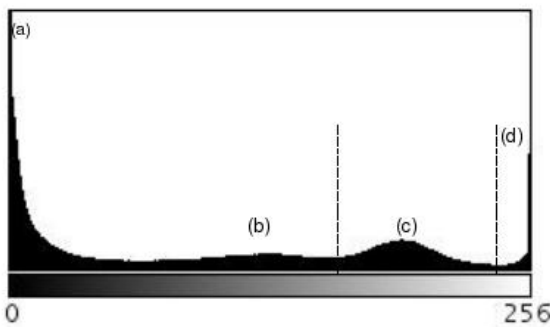

Fig. 2: Volume histogram from 3D filtered image corresponding to (a)background, (b)muscle, (c) liver and (d) bones. Two dash lines are local minimum between the highest peak.

the thresholding process. To remove these unwanted organs 3D connected component technique is used. This task is performed by examining the connectivity of voxels with their neighbors and assigning a unique label to each connected set found. The connected component algorithm presented in this work, assumes 26-connectivity for the foreground object. Only the maximum volume among all objects is selected, which further eliminated false liver regions.

IV. RESULTS AND DISCUSSION

The datasets used for the evaluation consists of 2D CT-slices obtained from Radiology Department, Hospital University of Freiburg. They consist of 25-30 slices with 512x512 resolution. The algorithm has been developed using C++ language in Linux environment. We conducted two experiments for visual analysis to confirm the usefulness of 3D anisotropic diffusion in helping the segmentation task.

First experiment is done by applying the 3D anisotropic diffusion to volumetric CT images and our result is shown in Fig. 3. Filtering was performed with five iterations with diffusion function c_1 and $\kappa = 5.0$. The result shows that after three iterations noise was significantly reduced, while the low-contrast edges between liver tissues and muscles tissues were enhanced. After five iterations, the intensities within the liver region are more uniform.

The next experiment conducted is to show the segmentation results using a thresholding technique with and without filtering step of 3D anisotropic diffusion. As shown in Fig. 4, it is easier to automatically find the optimal threshold values from the filtered images. Results from (d) and (h) clearly show that thresholding-based segmentation is enough to obtain initial liver region that has been isolated from adjacent organs. As a result, we do not need complex techniques for segmentation and also no need to incorporate a more priori knowledge for example, the location of the heart which is also difficult to identify. Different patients have different size and different shape of liver that can result in false localization.

Additionally, numerical analysis has been conducted on three datsets for which manual segmentation are available. It is evaluated using the volumetric overlap error [7] which is one of the most popular metric to evaluate segmentation. The volumetric overlap error measures the percentage of mismatching voxels between the automatic and manual segmentation. If V_S is a set of voxels from manual segmentation and V_A is a set of voxels from automatic segmentation, the percentage of volumetric overlap error between V_S and V_A is defined as

$$V_{oe} = 100 * \left(1 - \frac{|V_S \bigcap V_A|}{|V_S \bigcup V_A|}\right) \qquad (12)$$

If the percentage of volumetric overlap error is 0% it means a perfect segmentation is achieved. Otherwise, the more percentage of volumetric overlap error the less accurate of the segmentation result. We achieve between 15%–18% volumetric overlap error for our segmentation results although only 3D connected component process was performed for liver volume refinement.

Execution of the 3D anisotropic diffusion algorithm with five iterations took between 56.52s (25 slices) up to 71.5s (30 slices) on an Intel(R) Core(TM)2 Duo CPU with 3GHz and 7.7GB RAM.

V. CONCLUSION

The aim of this work is to show the advantages of using 3D anisotropic diffusion for helping in the liver segmentation task. The filter makes the intensities within the liver region more uniform. Thus, the filter can be used as a preprocessing step to a thresholding-based segmentation technique since the resulting images are simpler to segment than the originals. It is believed, if a proper liver volume refinement is performed, then the percentage of volumetric overlap error can be reduced. However, the drawback of this filtering method is that it requires more computational time due to the iterative process. Consequently, an appropriate parallel implementation of anisotropic diffusion is the best approach to reduce its execution.
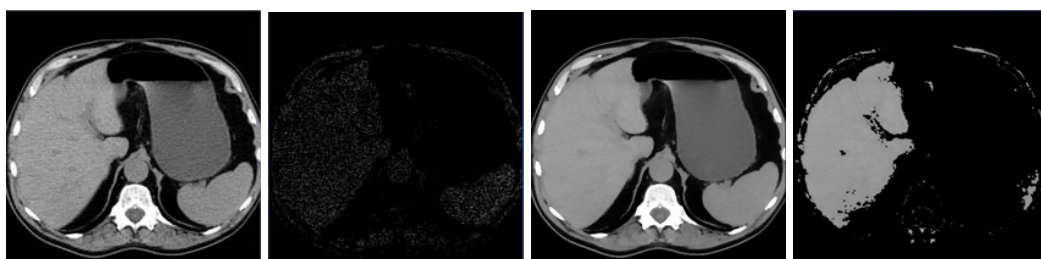
(a) Original image
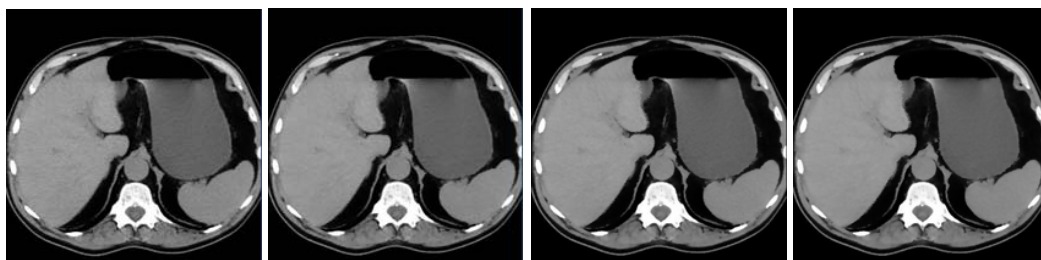
(b) after two iterations (c) after three iterations (d) after four iterations (e) after five iterations

Fig. 3: 3D anisotropic diffusion using diffusion function c_1 and $\kappa = 5.0$ after a number of iterations
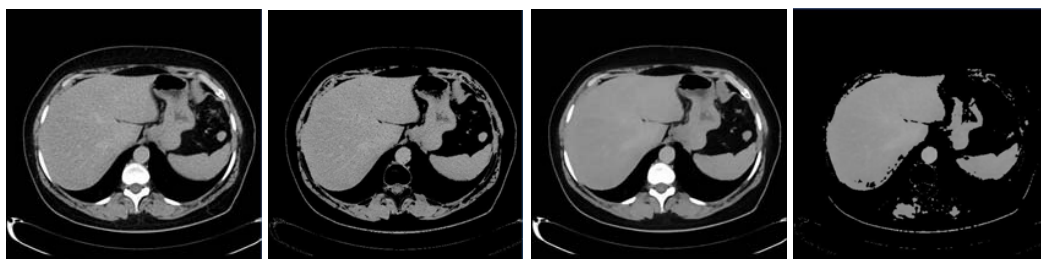

(a)   (b)   (c)   (d)

(e)   (f)   (g)   (h)

Fig. 4: Comparison of thresholding on the original image and filtered image. Top row: results from patient 1, (a) original, (b) result after thresholding from (a), (c) filtered image and (d) result after thresholding from (c). Bottom row: results from patient 2, (e) original, (f) result after thresholding from (e), (g) filtered image and (h) result after thresholding from (g).

REFERENCES

[1] A. Fenster and B. Chiu, Evaluation of segmentation algorithms for medical imaging, *Proceedings of the 2005 IEEE Engineering in Medicine and Bioloy 27th Annual Conference*, 2005, pp. 7186–7189.

[2] F. Liu, B. Zhao and P. K. Kijewski, Liver segmentation for ct images using gvf snake, *Medical Physics* 32, 2005, pp. 3699–3705.

[3] G. Gerig, O. Kübler, R. Kikinis and F. A. Jolesz, Nonlinear anisotropc filtering of MRI data, *IEE Trans. on Medical Imaging* 12, 1992, pp. 221–232.

[4] L. Massoptier and S. Casciaro, Fully automatic liver segmentation through graph-cut technique, *Proceedings of the 29th Annual International*, 007, pp. 5243–5246.

[5] P. Perona and J. Malik, Scale-space and edge detection using anisotropic diffusion, *IEEE Trans. on Pattern Analysis and Machine Intelligence* 12, 1990, pp. 629–639.

[6] S. J. Lim, Y. Y. Jeong and Y. S. Ho, Automatic liver segmentation for volume measurement in CT images. *Journal of Visual Communication and Image Representation* 17:4, 2006, pp. 860–875.

[7] T. Heimann, B. van Ginneken, M. Styner, Y. Arzhaeva, V. Aurich, C. Bauer, A. Beck, C. Becker, R. Beichel, G. Bekes, F. Bello, G. Binnig, H. Bischof, A. Bornik, P.M.M. Cashman, Y. Chi, A. Cordova, B.M.

Dawant, M. Fidrich, J. Furst, D. Furukawa, L. Grenacher, J. Hornegger, D. Kainmueller, R.I. Kitney, H. Kobatake, H. Lamecker, Th. Lange, J. Lee, B. Lennon, R. Li, S. Li, H.-P. Meinzer, G. Nemeth, D.S. Raicu, A.-M. Rau, E.M. van Rikxoort, M. Rousson, L. Rusko, K.A. Saddi, G. Schmidt, D. Seghers, A. Shimizu, P. Slagmolen, E. Sorantin, G. Soza, R. Susomboon, J.M. Waite, A. Wimmer, I. Wolf, Comparison and Evaluation of Methods for Liver Segmentation from CT datasets, *IEEE Transactions on Medical Imaging* in press. Digital Object Identifier 10.1109/TMI.2009.2013851.